Design of N-Path Switched-RC Narrow Band Bandpass Filter

A Project Report

submitted by

NIMIT JAIN

in partial fulfilment of the requirements
for the award of the degree of

BACHELOR OF TECHNOLOGY

under the guidance of
Dr. Shanthi Pavan

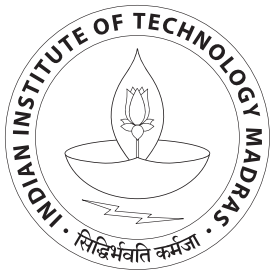

DEPARTMENT OF ELECTRICAL ENGINEERING
INDIAN INSTITUTE OF TECHNOLOGY, MADRAS.

May 2015

THESIS CERTIFICATE

This is to certify that the thesis entitled **Design of N-Path Switched-RC Narrow Band Bandpass Filter**, submitted by **Nimit Jain**, to the Indian Institute of Technology, Madras, for the award of the degree of **Bachelor of Technology**, is a bona fide record of the research work carried out by him under my supervision. The contents of this thesis, in full or in parts, have not been submitted to any other Institute or University for the award of any degree or diploma.

Dr. Shanthi Pavan
Project Guide
Professor
Dept. of Electrical Engineering
IIT-Madras, 600 036

Place: Chennai

Date:

ACKNOWLEDGEMENTS

I am extremely grateful to Prof. Shanthi Pavan for giving me the opportunity to work on this very interesting project. He has been an incredible mentor throughout the year and I could not have asked for more. He is truly an expert in noise shaping and has inculcated in me the habit of doing a neat job. I am also deeply indebted to him for teaching me EMC, Analog Circuits and Advanced Electrical Networks which propelled my fascination towards the Analog world.

I would like to thank Ashwin and the rest of the analog group for the help they provided me whenever I needed any clarifications. I would also like to thank Awanish who has helped me in designing the PCB and Anand Sir of IE Lab for helping me in carrying out the experiment.

And a big thank you to my friends. Thank you for being there not only to celebrate my success with me, but also for staying by my side during adversity.

I dedicate this thesis to my parents. Without their love, support and sacrifice none of this would have been possible.

ABSTRACT

The theory of N-Path filters is of a great practical importance as it provides an easy way of designing a highly frequency selective bandpass filter without usage of any magnetic or active-RC based elements. The most attractive trait of the N-Path filters is that the center frequency of the bandpass filter can be made independent of the circuit components and can be controlled externally by a clock. The main aim of this report is to provide a deep insight of this theory by bringing new perspectives into the picture. Simulation results are presented wherever possible. A simple model is also built to characterize the behavior of a practical narrow band which will aid the reader in building a bandpass filter effortlessly. This simple model matches closely with the simulated value. And based on this model, a narrow band bandpass filter of quality factor of 150 at the center frequency of 3.03KHz was built on a PCB.

TABLE OF CONTENTS

LIST OF FIGURES

ABBREVIATIONS

BPF Band Pass Filter

LPF Low Pass Filter

Q Quality factor

LTI Linear Time Invariant

LPTV Linear Periodically Time Varying

DC Direct Current (Zero frequency)

PAC Periodic AC

HTF Harmonic Transfer function

ATF Aliasing Transfer function

SE Single Ended

DE Differential Ended

DFT Discrete Fourier Transform

DSO Digital Storage Oscilloscope

CHAPTER 1

Introduction

1.1 Motivation and Objectives of the Thesis

A tunable highly frequency selective bandpass filter is desired in almost all the communication devices. A passive RC circuit can never give this kind of filtering as all the poles of a passive RC network lie on negative real axis. Inductors are usually avoided in pratice as they are bulky. By using active-RC based configuration we can mimic the role of an inductor. But when we make an endeavor to realize a high Q filter, we run into problems of system stability. Even if we are able to make a stable bandpass filter, it would be extremely hard to tune this filter without changing the bandwidth of the filter. We can evade from these problems by using an N-Path filter.

The N-Path filter is an LPTV system which under certain conditions can be made to look like an LTI system. If the component network of each path is a lowpass filter then the N-Path filter exhibits comb filter like characteristic. This periodic filtering or comb filter like characteristic can be made to look like a BPF by applying by eliminating all other passbands other than the desired one using a broad bandpass filter. The N-Path essentially transforms the low-pass behavior to a higher frequency which is the usually the beat frequency of this LPTV system. This beat frequency doesn't depend on any of the internal components and can be controlled externally. This is how we can generate a tunable narrowband BPF.

The objectives of this thesis are as follows:

- To spur the interest of the reader in the N-Path filters for designing a BPF.
- To derive all the equations governing this system either by mentioning in the report or directing to a reference and then showing the corresponding result from the circuit simulator (Cadence Spectre Circuit Simulator).
- To build a simple model for the transfer function of a practical BPF circuit around the center frequency.
- To mention the practical challenges associated with the design of N-Path filters.
- To describe the experimental procedure used in designing a BPF with the center frequency of 3.03KHz and band width of 20Hz.

1.2 Structure of the thesis

Chapter 2 describes the theory of N-Path filter presented in [1] in detail. We have first started with building a BPF from a single path and showed that it cannot be used. Then we have constructed the BPF using two paths and showed why it works. After understanding why the two path filter worked we have built an N-Path filter. But the realization of these filters needed an accurate multiplier circuit and sinusoidal modulator. To overcome this problem we have introduced the N-Path sampled data networks.

Chapter 3 introduces a practical circuit to implement the BPF. We have developed a simple model to understand the transfer function of this circuit using the theory of N-Path filter developed in Chapter 2. We have also explained how to build a DE filter by following [2] which is more suitable for practical purposes than its SE counterpart.

Chapter 4 deals with the design of the BPF using the model developed in chapter 2. In this chapter we have shown that the experimental results match with the simulated results.

CHAPTER 2

The Theory of N-Path Filters

2.1 Need for More than One Path to Design a Narrow Band BPF

As designing a narrow band BPF response using an LTI system is quite challenging, one commonly used technique is to down convert the input signal to base band, send it to a LPF and then up convert it. This is shown in the Fig. 2.1. This configuration works only if the input signal is symmetric about the center frequency f_0. If the signal is unsymmetrical about f_0(1MHz), as shown in Fig. 2.2a, and is passed to this single path BPF filter which contains an ideal LPF H(f) of bandwidth 30KHz, the output we get is shown in Fig. 2.2b.

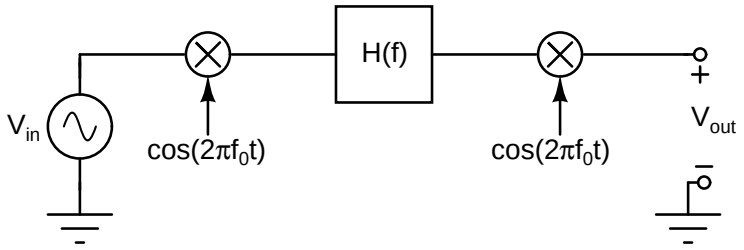

Figure 2.1: Single path BPF

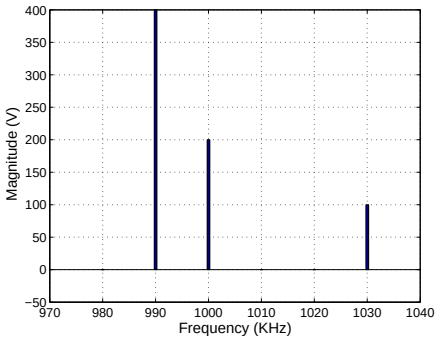

(a) DFT of the input

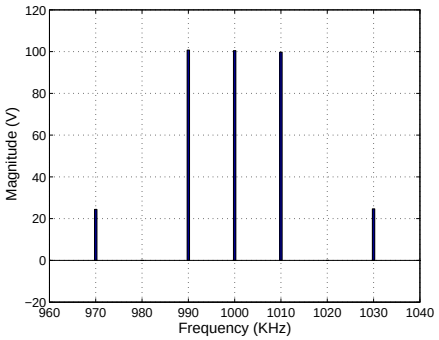

(b) DFT of the output

Figure 2.2: Response of the single path filter

Ideally, we wanted our BPF to give the same gain for all the frequencies in the desired band and attenuate all other frequencies. But in the output spectrum, we see unwanted components at 970KHz

and 1010KHz. The signal at 990KHz, which was double the strength of the signal at 1MHz appears to have the same strength in the output spectrum. This kind of behavior is quite obvious once we write the Fourier transform of the output in terms of the input and is given as follows:

$$V_{out}(f) = \frac{1}{4}(V_{in}(f-2f_0)H(f-f_0)+V_{in}(f)(H(f-f_0)+H(f+f_0))+V_{in}(f+2f_0)H(f+f_0)) \quad (2.1)$$

At frequency $f_0+\Delta f$ (assuming H(f) to be a brick wall filter with cut-off frequency much smaller than f_0), the output voltage is:

$$V_{out}(f_0+\Delta f) = \frac{1}{4}(V_{in}(-f_0+\Delta f)+V_{in}(f_0+\Delta f)) \quad (2.2)$$

As the input is a real signal, $V_{in}(f) = V_{in}(-f)$

$$V_{out}(f_0+\Delta f) = \frac{1}{4}(V_{in}(f_0-\Delta f)+V_{in}(f_0+\Delta f)) \neq C(V_{in}(f_0+\Delta f)) \quad (2.3)$$

So, the output voltage gets distorted if the input voltage is not symmetric about the center frequency. In the expression for the output voltage, the undesired terms are $\frac{1}{4}(V_{in}(f-2f_0)H(f-f_0)$ and $\frac{1}{4}V_{in}(f+2f_0)H(f+f_0)$. To get rid of these terms we could use a two path approach. The motivation for this technique comes from the concept of complex base-band equivalent of a pass-band signal [3]. In the two path approach, the modulators in the second path have a phase difference of $\frac{\pi}{2}$ radians with respect to those in the first path. The block diagram is shown in the Fig. 2.3. The corresponding output is given in the Fig. 2.4.

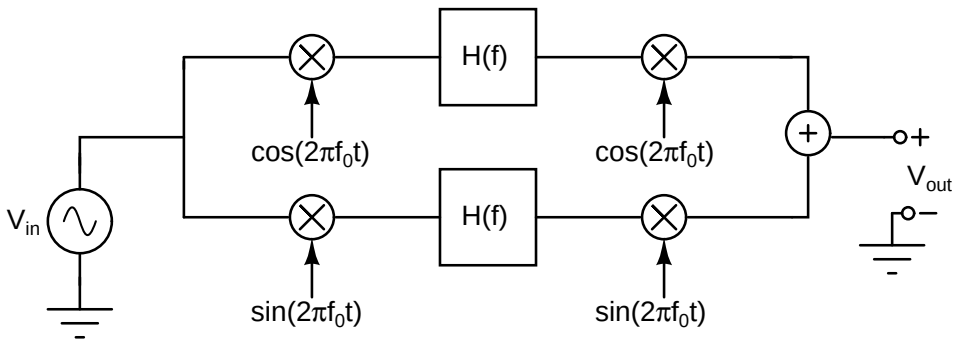

Figure 2.3: Two path BPF

We have already seen the expression of the output of the first path. For the second path, the expression for the output is given as follows:

$$V_{out,2}(f) = \frac{1}{4}(-V_{in}(f-2f_0)H(f-f_0)+V_{in}(f)(H(f-f_0)+H(f+f_0))-V_{in}(f+2f_0)H(f+f_0)) \tag{2.4}$$

Adding the output of both the paths eliminates the undesired terms and we get the transfer function of a BPF. Moreover, the system now looks like an LTI one.

$$V_{out}(f) = \frac{1}{2}V_{in}(f)(H(f-f_0)+H(f+f_0)) \tag{2.5}$$

2.2 N-path filter with Sinusoidal Modulators

In the two path case, we have seen that the undesired components add destructively in phase and the desired component adds constructively to give an LTI system like behavior. N-path filter is the extension of this simple concept.

The block diagram of the N-path filter using sinusoidal modulators is given in Fig. 2.5. Here again there is phase difference between the modulators. The phase difference between two consecutive modulators is $\frac{2\pi}{N}\tau$ where $\tau = \frac{1}{f_0 N} = \frac{T_0}{N}$. The N-path filter reduces to the 2-path filter for the value of N equal to 4. In this case, the third path is same as the first path and, the fourth path is same as that of the second path. After removing these two redundant paths, the 4-path system reduces to the 2-path filter discussed above.

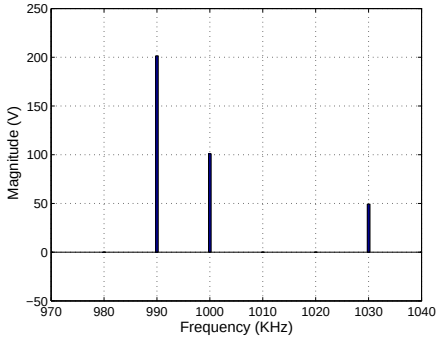

Figure 2.4: Output of two path filter

Now, we shall discuss how cancellation of undesired terms occurs in the N-path. The output of the nth path ($v_n(t)$) in the Fig. 2.5 can be expressed in terms of input by the following relation:

$$V_n(f) = \frac{1}{4}(U(f-2f_0)H(f-f_0)e^{-j\frac{4\pi(n-1)}{N}} + U(f)(H(f-f_0)+H(f+f_0)) + U(f+2f_0)H(f+f_0)e^{j\frac{4\pi(n-1)}{N}}) \tag{2.6}$$

We know that $e^{-j\frac{2\pi(n-1)}{N}}$, n going from 1 to N are the N roots of unity. And also, the sum of squares of the N roots of unity equals zero. So, on summing the output of each path, the undesired terms cancel out. Giving:

$$V(f) = \frac{N}{4}U(f)(H(f-f_0) + H(f+f_0)) \tag{2.7}$$

the transfer function of a BPF. The LPF H(f) is now transformed to a BPF. The striking feature of the N-Path filter is that the center frequency of the BPF doesn't depend on the component network.

This result was verified using the PAC analysis of the circuit simulator Cadence Spectre. A 5-path filter was used and is shown in 2.6a. The zeroth sideband of the output was plotted and is shown in Fig. 2.6b. From the plot we can notice that the shape of the BPF around the center frequency (4KHz) is same as that of the LPF around DC.

2.3 General N-path filter

Practically, it is very difficult to realize both an accurate multiplier circuit and a sinusoidal modulator of a constant frequency. If we could use square wave modulator instead of sinusoidal one, then we can

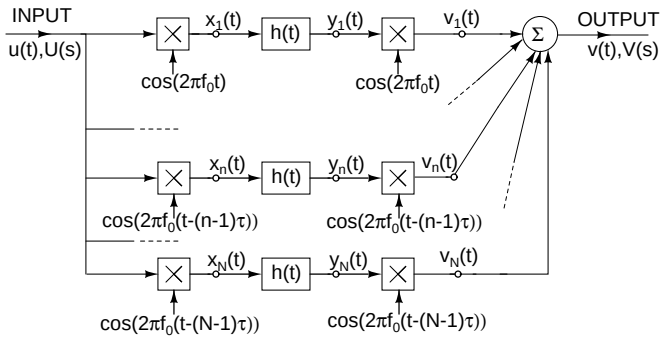

Figure 2.5: Block diagram of N-path filter with sinusoidal

realize the multiplier circuit using a simple switch circuit. This motivates us to see what happens if the modulator is square wave. As a square wave contains infinite harmonics, we first consider the case when the modulators contain only two harmonics and then generalize to case when it has infinite harmonics.

Consider the path shown in Fig. 2.7. Here I have shown a path in which the modulator has a delay τ with respect to the first path. The output of this path comprises of 9 terms and is given as follows:

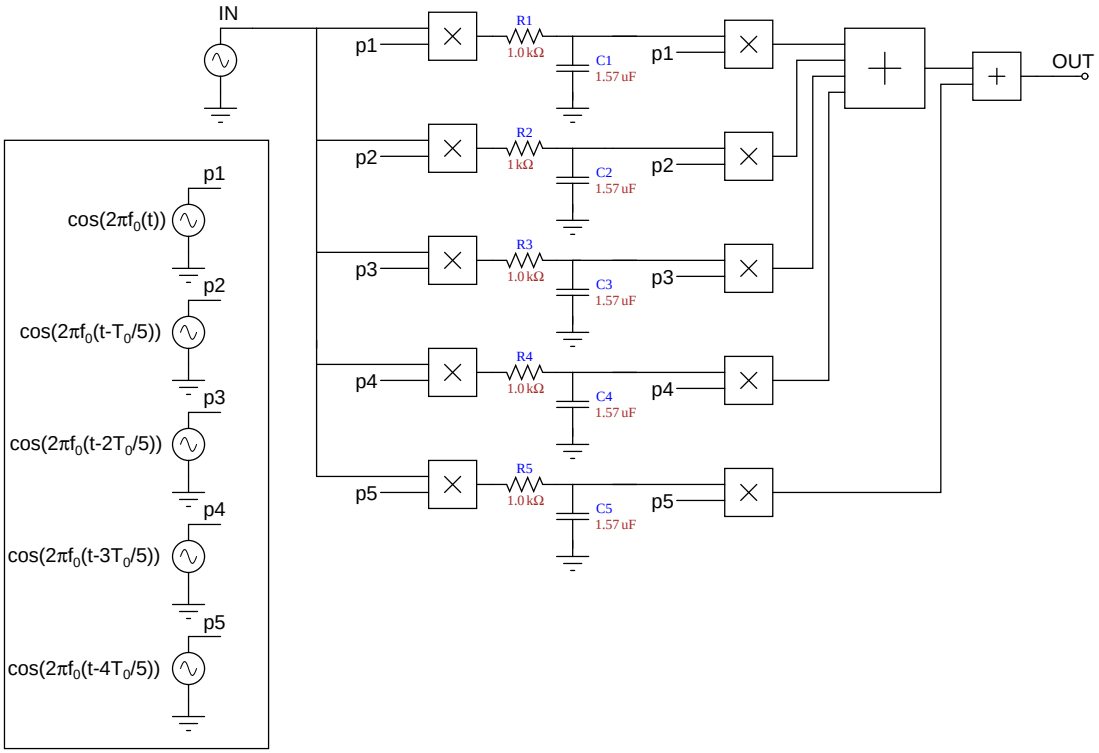

(a) Circuit diagram

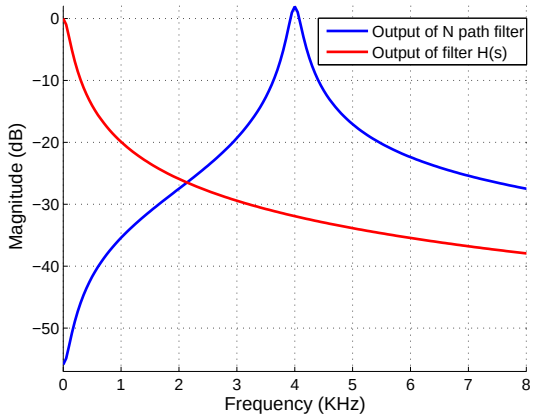

(b) Simulation result

Figure 2.6: Low-pass to bandpass conversion

$$V(f) = \sum_{k=-4}^{4} P_k(f)U(f - kf_0)$$

$P_k(f)$ are given as follows:

$P_4(f) = \frac{A_2^2}{4}e^{-j8\pi f_0\tau}H(f - 2f_0)$

$P_3(f) = \frac{A_1A_2}{4}e^{-j6\pi f_0\tau}H(f - f_0) + \frac{A_1A_2}{4}e^{-j6\pi f_0\tau}H(f - 2f_0)$

$P_2(f) = \frac{A_1^2}{4}e^{-j4\pi f_0\tau}H(f - f_0)$

$P_1(f) = \frac{A_1A_2}{4}e^{-j2\pi f_0\tau}H(f - f_0) + \frac{A_1A_2}{4}e^{-j2\pi f_0\tau}H(f - 2f_0)$

$P_0(f) = \frac{A_1^2}{4}(H(f - f_0) + H(f + f_0)) + \frac{A_2^2}{4}(H(f - 2f_0) + H(f + 2f_0))$

$P_{-1}(f) = \frac{A_1A_2}{4}e^{j2\pi f_0\tau}H(f + f_0) + \frac{A_1A_2}{4}e^{j2\pi f_0\tau}H(f + 2f_0)$

$P_{-2}(f) = \frac{A_1^2}{4}e^{j4\pi f_0\tau}H(f + f_0)$

$P_{-3}(f) = \frac{A_1A_2}{4}e^{j6\pi f_0\tau}H(f + f_0) + \frac{A_1A_2}{4}e^{j6\pi f_0\tau}H(f + 2f_0)$

$P_{-4}(f) = \frac{A_2^2}{4}e^{j8\pi f_0\tau}H(f + 2f_0)$

When τ equals $(n-1)T/N$ the delay between the modulator of the nth path from the first path, the phase term ($e^{-j8\pi f_0\tau}$) in $P_{\pm4}(f)$ equals one for the value of N equal to 4. Now, if we sum over all the paths, we not only get P_0(f) but also $P_{\pm4}$(f). The rest of the terms cancel on summation. Also, we observe that the desired transfer function P_0(f) now has two pass bands, i.e at f_0 and at $2f_0$. Fig 2.8 shows the schematic and simulation result.

From the two harmonic case, we have observed that as the number of harmonics increase, the side-bands which are multiples of number of paths (N) do not vanish after summation. Also, the transfer function will contain more than one passbands. If the modulators contain M harmonics, the output of each path will have sidebands ranging from -2M to 2M. Out of these (2M+1) sidebands, the sidebands

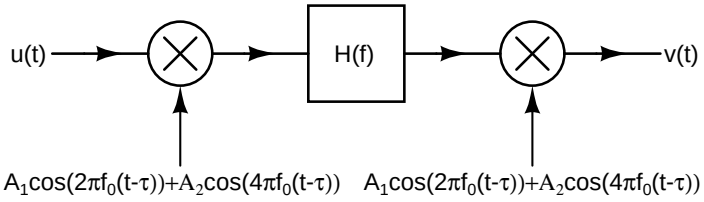

Figure 2.7: Modulators as sum two harmonics

which are multiples of N will not vanish on summation. The desired transfer function or the zeroth sideband will now contain M passbands. To get rid of the undesired sidebands, one can choose the value of N to be greater than 2M.

In a more general case, when the input and output are periodic functions p(t) and q(t) as shown in Fig. 2.9. The input and output relation is given by the following equation: [1]

$$V(f) = \sum_{k=-\infty}^{\infty} F_k(f)U(f - kNf_0) \tag{2.8}$$

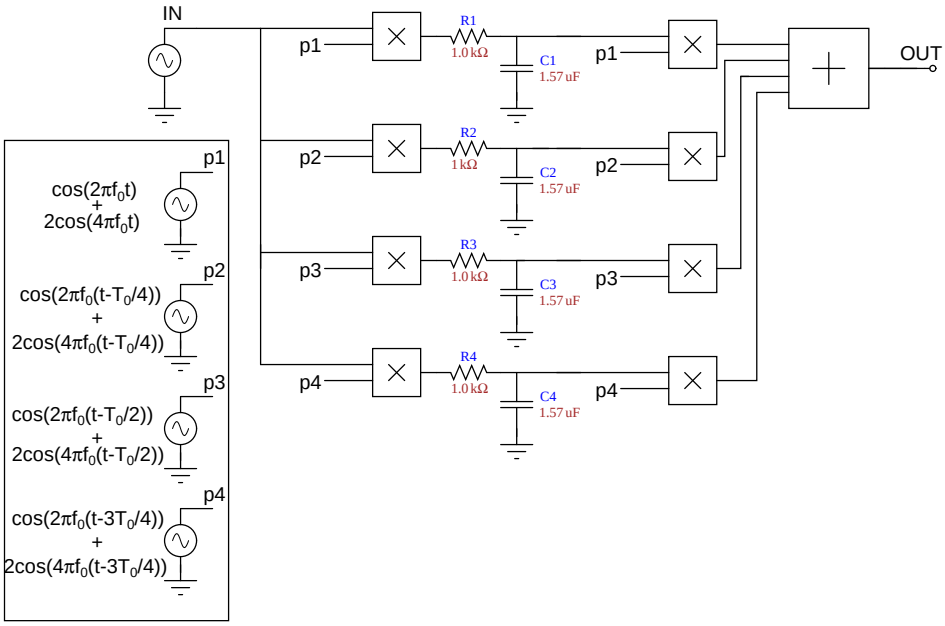

(a) Schematic

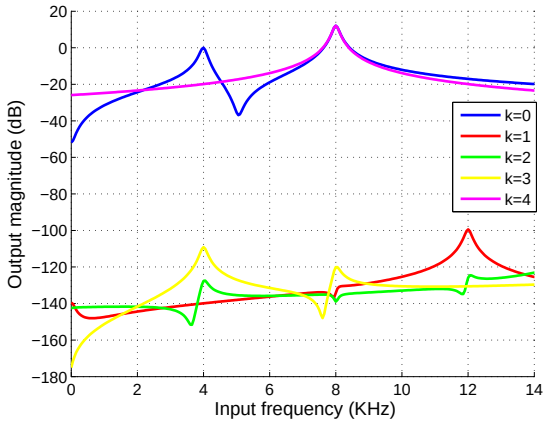

(b) Simulation result

Figure 2.8: Simulation of N-path filter with modulator as sum of two harmonic

$$F_k(f) = N \sum_{l=-\infty}^{\infty} P_{kN-l} Q_l H(f - lf_0) \tag{2.9}$$

Where P_{kN-l} and Q_l are the kN-l^{th} and l^{th} Fourier series coefficients of the periodic functions p(t) and q(t) respectively. The eq. 2.8 says that the N-path filter is an LPTV system which contains sidebands only at the multiples of N. If we band limit the input and output to $Nf_0/2$, then the LPTV system collapses to an LTI system with the transfer function given below:

$$T(f) = \frac{V(f)}{U(f)} = F_0(f) \; for \; |f| < \frac{Nf_0}{2} \tag{2.10}$$

$$= 0 \; otherwise \tag{2.11}$$

Band-limiting can be done by applying a LPF both at the input and the output. The equivalent block diagram is shown in Fig. 2.10. Eq. 2.9 conveys that when H(f) has a LPF characteristic, the transfer function T(f) behaves like a comb filter.

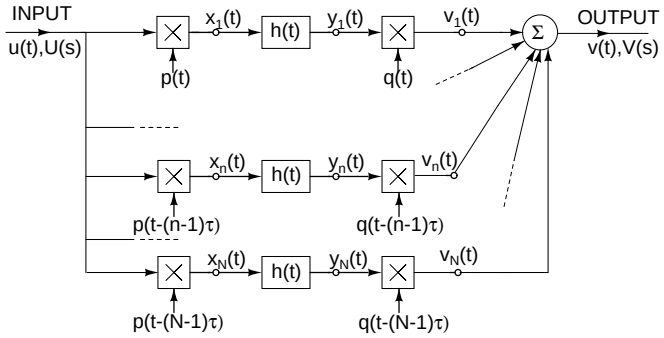

Figure 2.9: General N-path filter

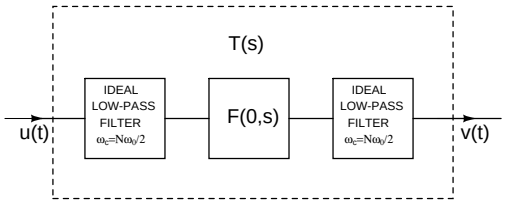

Figure 2.10: Equivalent block diagram of the N-path filter

2.4 N-path sampled data network

We have seen the relation between the input and output when the modulators are periodic signals in the previous section. If we take the case when both the modulators p(t) and q(t) are square waves, the task of multiplication of input with p(t) reduces to the placement of a switch (controlled by the clock p(t)) in the path of input . This simplification is valid only when the input is a current source. Moreover, the operation of switching is equivalent to multiplying with an impulse train, if the on time (d) of switches is much smaller than the time period. We are effectively sampling the input data. And so, the N-path filter with switches is called N-path sampled data network in the literature [1]. To model this system, the modulator p(t) can be written as:

$$p(t) = q(t) = d \sum_{k=-\infty}^{\infty} \delta(t - kT_0) \tag{2.12}$$

Now we find the input-output relation for the N-path sampled data network.

$$x_n(t) = d \sum_k u(kT_0 + \overline{n-1}\tau)\delta(t - (kT_0 + \overline{n-1}\tau)) \tag{2.13}$$

$$y_n(t) = d \sum_k u(kT_0 + \overline{n-1}\tau)h(t - (kT_0 + \overline{n-1}\tau)) \tag{2.14}$$

$$v_n(t) = d^2 \sum_m \sum_k u(kT_0+\overline{n-1}\tau)h((mT_0+\overline{n-1}\tau)-(kT_0+\overline{n-1}\tau))\delta(t-(mT_0+\overline{n-1}\tau)) \tag{2.15}$$

$$v_n(t) = d^2 \sum_m \sum_k u(kT_0 + \overline{n-1}\tau)h((m-k)T_0)\delta(t - (mT_0 + \overline{n-1}\tau)) \tag{2.16}$$

To get a better understanding, we define the following:

$u_n[m] = u(mT_0 + \overline{n-1}\tau)$

$h[m] = h(mT_0)$

$v_n[m] = u_n[m] * h[m]$

After substituting these in the above equation, we get:

$$v_n(t) = d^2 \sum_m v_n[m]\delta(t - (mT_0 + \overline{n-1}\tau)) \tag{2.17}$$

$$v(t) = \sum_{n=1}^{N} v_n(t) \tag{2.18}$$

A careful observation on the above equations suggests that the system can be modeled as a digital system shown in Fig. 2.11 (except for the d^2 factor). Now we shall explain the reason behind this. If we sample the input at the rate Nf_0 and we call it u[m], then u[m] is given by:

$$u[m] = u(m\frac{T_0}{N}) \tag{2.19}$$

Then if we pass u[n] to advance block z^{n-1}, we get:

$$u_{adv}[m] = u[m+n-1] = u((m+\overline{n-1})\frac{T_0}{N}) \tag{2.20}$$

Then after passing through the decimation filter we get:

$$u_{dec}[m] = u[Nm] \tag{2.21}$$

$$= u(mT_0 + \overline{n-1}\frac{T_0}{N}) \tag{2.22}$$

The value of u_{dec}[m] equals u_n[m] defined above. If we sample the impulse response of the filter H(f) we get h[m] defined above. The Z-transform of h[m] is H(z) shown in the block diagram. When u_{dec} is passed through the filter H(z) we get $u_{dec} * h$ which equals v_n[m]. Then following the process shown in the Fig. 2.11, the output we get is sampled version of v(t) at the rate Nf_0.

This model is valid only if the bandwidth of input signal is less than $\frac{Nf_0}{2}$ (to avoid aliasing as input is sampled at Nf_0). The system shown can be reduced using noble identities [4] of multirate system as shown in 2.12. If H(z) is a LPF, $H(z^N)$ gives the characteristic of a comb filter. The N-path sampled data network essentially takes the block H(z) and converts it into $H(z^N)$.

2.5 Narrow Band BPF Design Using N-Path Sampled Data Network

To implement N-path sampled data network, we need current source at the input and no load at the output. It was shown by Franks and Sandberg [1] that this problem can be alleviated by forcing one additional constraint into the system. Fig. 2.13 shows the scenario when a source having impedance R1 is passed to a N-path sampled data network with load R2. The broad band BPF at the output is placed to reject all the pass bands other than the one at f_0. The two port network in each path is described using the two port parameters Z(f) instead of transfer function H(f). It was shown in [1] that if $Z_{ij}(f)$ vanishes for $|f| > f_0/2$, then the transfer function becomes:

$$T(f) = \frac{E_2(f)}{E_1(f)} = \frac{Nd_2}{T}[a_1 G(f - f_0) + \overset{*}{a_1} G(f + f_0)] \tag{2.23}$$

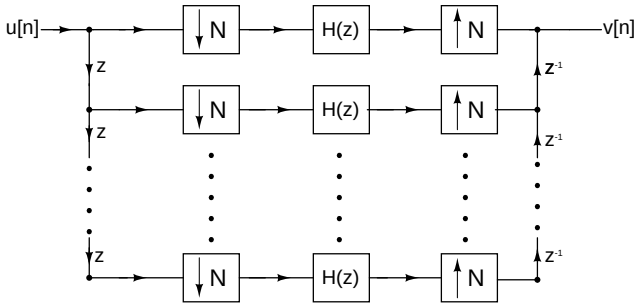

Figure 2.11: Digital equivalent of N-path filter

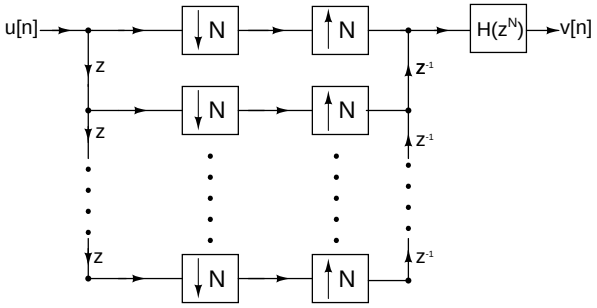

(a) Shifting H(z) to the right using noble identity

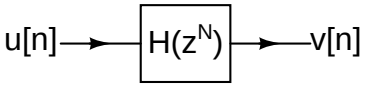

(b) The equivalent single path after final reduction

Figure 2.12: Block reduction of digital N-path filter model

where,

$d_1$and d_2 are the on times of the switching block at the input and output respectively.

$a_1 = e^{j(\pi/T)(d_1-d_2)}(\frac{\sin\frac{\pi d_1}{T}}{\frac{\pi d_1}{T}})(\frac{\sin\frac{\pi d_2}{T}}{\frac{\pi d_2}{T}})$

G(f) is the transfer function from V_1 to V_2 as shown in Fig. 2.14.

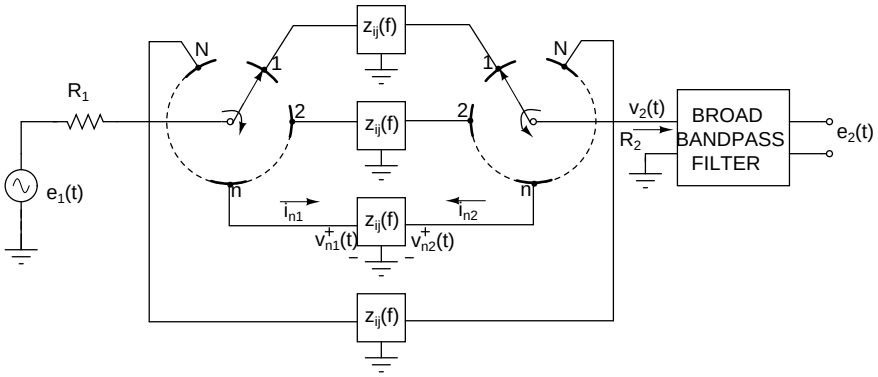

Figure 2.13: Practical N-Path filter

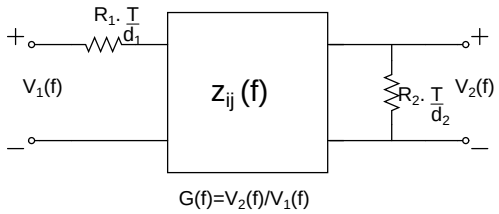

Figure 2.14: Equivalent LPF network

To verify this result, the circuit diagram used in [1] which is shown in Fig. 2.15a. was used to observe the output. Fig. 2.15c shows the zeroth sideband around the center frequency 25KHz. The quality factor of this circuit was 3289.

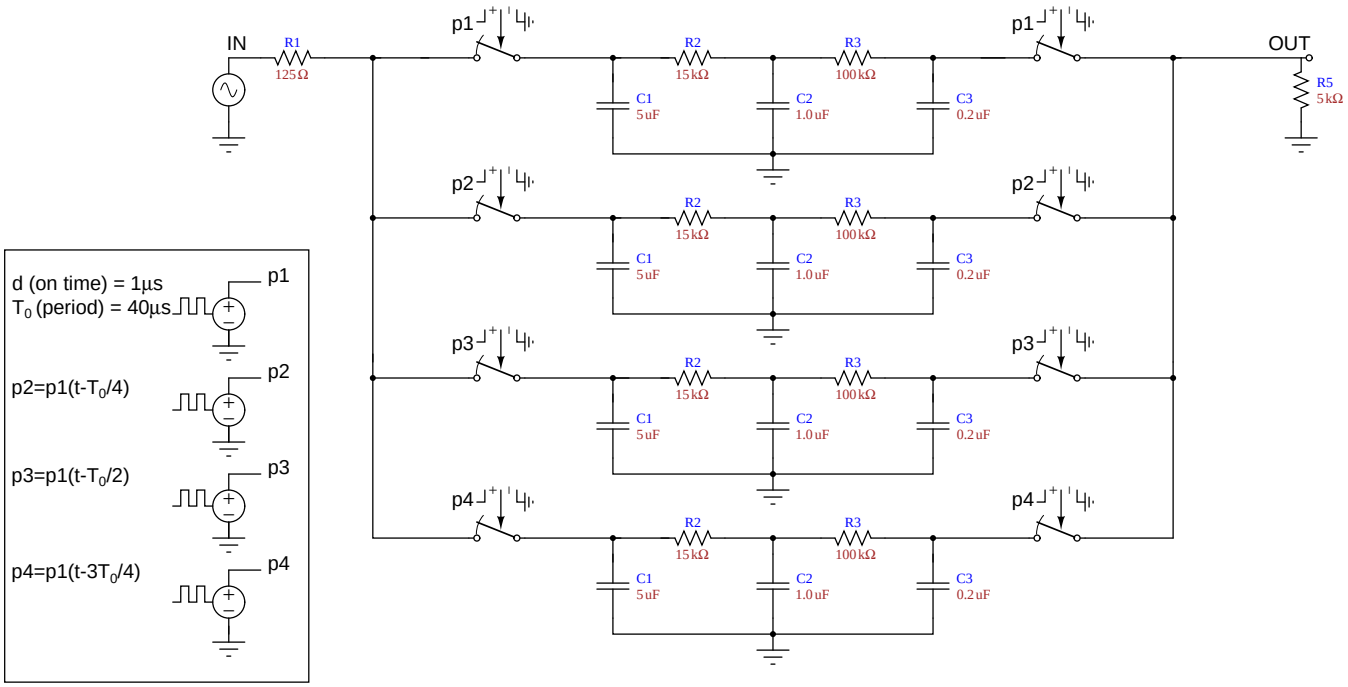

(a) Schematic

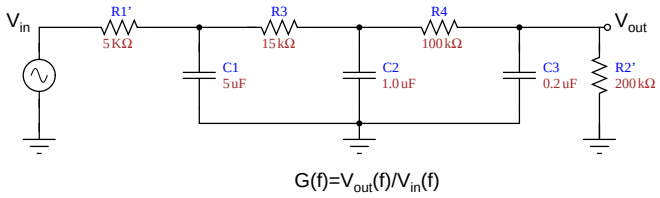

(b) Equivalent LPF network

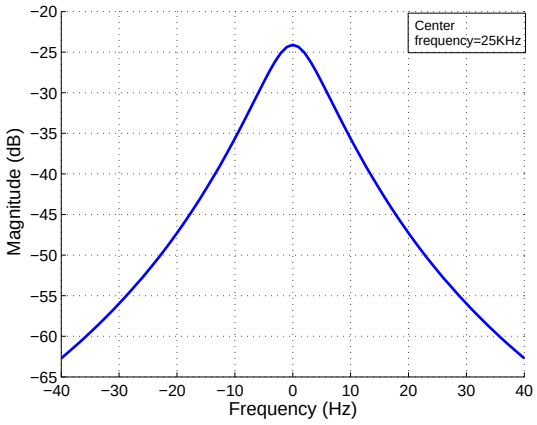

(c) Magnitude response of the transfer function

Figure 2.15: Practical Narrow band BPF

CHAPTER 3

Practical Design of Narrow Band BPF

3.1 Practical BPF Circuit

In the previous section we have seen how to design a BPF which has finite input and output impedance. The chief limitation of the that configuration is the usage of impulse sampling. There is one another model for BPF which is quite popular in the literature. This circuit is shown in Fig. 3.1(a). Here the switches $S_{i1}$and S_{i2} (i goes from 1 to N) have the same on and off time. The circuit can be reduced to a simpler circuit shown in 3.1(b). This simplification follows from the observation that the resistors are active only when the switches are closed. Please note that if the resistors were in parallel with the capacitors then we couldn't have taken them outside. This is because, when the switches close the resistors are still active as they drain out the capacitors. As this doesn't happen with the configuration shown in Fig. 3.1(a), we can safely take the resistor outside of its left switch . Also, as the switches are assumed to have non-overlapping on time, a single resistor will serve the purpose.

3.2 SE Circuit Analysis

To find the exact transfer function of the SE BPF shown in Fig. 3.1 one could refer [5] which, however, is very complicated in nature. We'll first explain how the sideband cancellation occurs for this network and then develop a simple model to characterize the behavior of the system. We would also like to point out that when all are switches are turned off, the output simply tracks the input. To prevent this, we have made a small modification and is shown in the Fig. 3.2. R_{Load} is chosen high enough to not effect the rest of the circuit when a particular switch (other than S_0) is on. It behaves like an open circuit when the switches are turned on and gives a zero voltage when all the switches are turned off.

The N-path filter can now decomposed as a sum of N independent LPTV systems as shown in Fig. 3.3. This was possible only after addition of the switch S_0 and a high impedance R_{Load}. We know that the output of a LPTV system can be written in the following form: (slightly different from the one shown in [5]

$$V_{out}(f) = \sum_{m=-\infty}^{\infty} H_m(f) V_{in}(f - mf_0) \tag{3.1}$$

where f_0 is the frequency at which the system is periodic and $H_m(f)$ s are the harmonic transfer functions. If we advance the time axis of k^{th} LPTV system by σ_k (σ_k=kT/N for k going from 0 to N-1) in Fig. 3.3, then switching action will be done at the same time in all the N LPTV systems. The input to the k^{th} LPTV system after advancing is denoted by $\hat{v}_{in}(t)$ and the output by $\hat{v}_{out}$. The input-output relation can be obtained from the following:

$$\hat{v}_{in}(t) = v_{in}(t + \sigma_k) \tag{3.2}$$

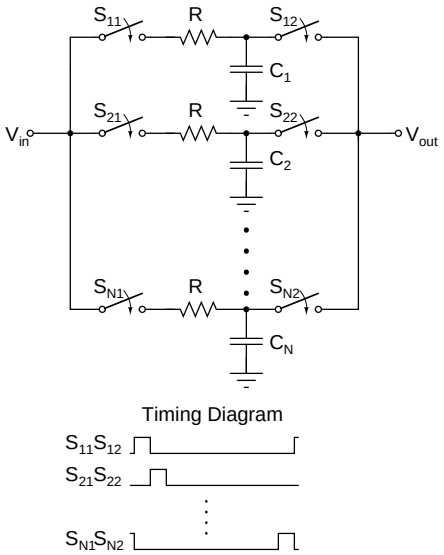

(a) SE switched-RC N-path filter

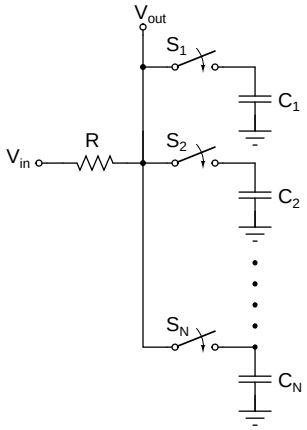

(b) Simplified circuit

Figure 3.1: Practical BPF circuit

$$\hat{v}_{out,k} = v_{out,k}(t + \sigma_k) \tag{3.3}$$

$$\hat{V}_{out,k}(f) = \sum_m H_{m,k}(f)\hat{V}_{in}(f - mf_0) \tag{3.4}$$

As switching occurs at the same time, all the N paths will have the same HTF $H_{m,0}(f)$. Taking the Fourier transform of the eqs. (3.2,3.3)

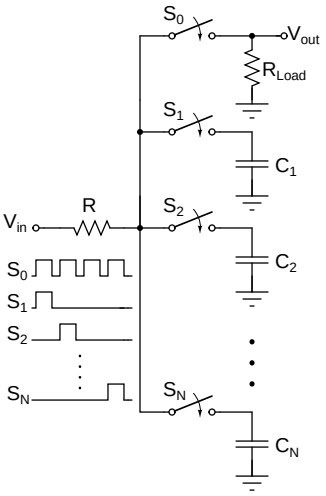

Figure 3.2: Practical SE N-path filter

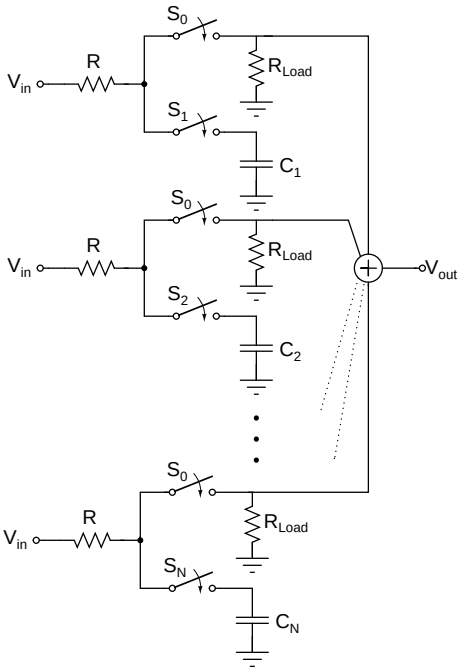

Figure 3.3: Equivalent model of N-path filter as sum N independent LPTV systems

$$V_{out,k}(f) = \sum_m H_{m,0}(f) V_{in}(f - mf_0) e^{-j2\pi m f_0 \sigma_k} \tag{3.5}$$

As the output is sum of all the LPTV blocks,

$$V_{out}(f) = \sum_{k=0}^{N-1} V_{out,k}(f) \tag{3.6}$$

$$= \sum_m H_{m,0}(f) V_{in}(f - mf_0) \sum_{k=0}^{N-1} e^{-j2\pi m f \sigma_k} \tag{3.7}$$

$$= \sum_m H_{m,0}(f) V_{in}(f - mf_0) \sum_{k=0}^{N-1} e^{-j2\pi m f_0 kT/N} \tag{3.8}$$

Clearly, all the values of m which are not a multiple of N vanish, giving us:

$$V_{out}(f) = \sum_n H_n(f) V_{in}(f - Nnf_0) \tag{3.9}$$

where $H_n(f)=NH_{Nn,0}$. So we have shown the sidebands cancellation property. Please note that we have not constrained the switching to happen instantaneously so far. Just ensuring the same duty cycle in the clocks of all the switches will make the sidebands which are not multiples of N to vanish. If we now restrict $V_{in}(f)$ to lie in the frequency range $-Nf_0/2$ to $Nf_0/2$, then the sidebands won't interfere with each other. And if we apply a LPF at the output of cutoff frequency $Nf_0/2$, then

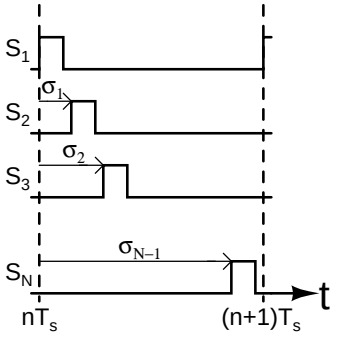

Figure 3.4: Timing diagram

$$V_{out}(f) = H_0(f)V_{in}(f) \tag{3.10}$$

Now we shall determine a simple expression for $H_0(f)$ of this network. For this we constrain switching to happen instantaneously. If the current flowing out of the input is i(t) and if the duty cycle of the clocks S_1 to S_N is 1/N (instantaneous switching), then

$$v_{out}(t) = v_{in}(t) - i(t)R \tag{3.11}$$

$$V_{out}(f) = V_{in}(f) - I(f)R \tag{3.12}$$

The relation between the I(f) and $V_{out}(f)$ can be obtained easily as they are the input and output respectively in the general N-path filter structure mentioned in the previous chapter. From the Fig. 3.5,

$$V_{out}(f) = \sum_k F_k(f)I(f - kNf_0) \tag{3.13}$$

$$F_k(f) = N\sum_l P_{-l}P_l \frac{1}{j2\pi(f - f_0 l)C} \tag{3.14}$$

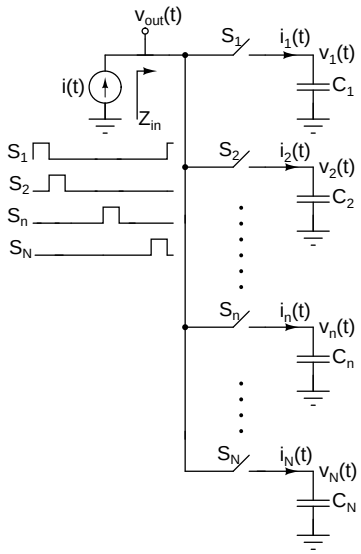

Figure 3.5: General N-path structure with input as i(t) and output as $v_{out}(t)$

where P_l is the Fourier series coefficient of a periodic pulse of width T_0/N and width T_0 ($T=1/f_0$).

$F_0(f)$ is also the looking in impedance when all the other sidebands were absent and is denoted by $Z_{in}(f)$.

From eqs. (3.10,3.12):

$$V_{out}(f) = \frac{V_{out}(f)}{H_0(f)} - RI(f) \tag{3.15}$$

$$V_{out}(f) = (\frac{H_o}{1 - H_0})RI(f) \tag{3.16}$$

The validity of the above expression may not hold when $H_o(f)$ equals zero or one.

By comparing eq (3.13,3.16), we conclude that because of applying lowpass filter all the sidebands except at zero vanish and we get:

$$(\frac{H_o}{1 - H_0})R = Z_{in}(f) = N \sum_l P_{-l} P_l \frac{1}{j2\pi(f - f_0 l)C} \tag{3.17}$$

$$H_o(f) = \frac{N \sum_l P_{-l} P_l \frac{1}{j2\pi(f - f_0 l)RC}}{1 + N \sum_l P_{-l} P_l \frac{1}{j2\pi(f - f_0 l)RC}} \tag{3.18}$$

When f is close to f_0, then the term l =1 dominates and we get:

$$H_0(f) \approxeq \frac{N|P_1|^2 \frac{1}{j2\pi(f - f_0)RC}}{1 + N|P_1|^2 \frac{1}{j2\pi(f - f_0)RC}} \tag{3.19}$$

$$= \frac{1}{1 + j2\pi(f - f_0)R\hat{C}} \tag{3.20}$$

where $\hat{C}$ equals $\frac{C}{N|P_1|^2}$.

And at f = f_0+$1/(2\pi R\hat{C})$, the magnitude of the output voltage falls by 3dB. Therefore, the bandwidth of the BPF is:

$$BW = \frac{1}{\pi R\hat{C}} \tag{3.21}$$

Fig. 3.6 shows the comparison between theoretical model (eq. 3.20) and zeroth sideband obtained using PAC analysis from the circuit simulator around the center frequency of 3.03KHz. We can see that

the model matches closely with the simulated value. However, the value at the center frequency from simulation is about 0.8dB lesser than the expected value but matches at other points close to the center frequency. So the calculated bandwidth will be lesser than the one obtained from simulation. The true value of transfer function at f_0 can be obtained from the formula given in [2] after substituting n = 1 and D = 1/N and is given as follows:

$$H_0(f_0) \approx (\frac{\sin(\frac{\pi}{N})}{\frac{\pi}{N}})^2 \tag{3.22}$$

Also at frequencies away from the center frequency we see deviation of the simulated model from the theoretical model. This can be rectified by adding the terms at l=0 and l=2 from the eq. 3.18.

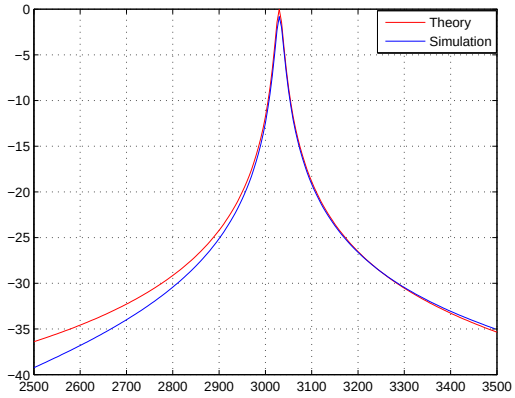

Figure 3.6: Comparison of theoretical model with output from simulation

3.3 DE Circuit Analysis

3.3.1 Derivation of the Transfer Function

From a practical perspective, DE circuits have a great advantage over their SE counterparts. The common mode error in SE circuit can be eliminated by using a DE circuit. For our application of designing a BPF, we can exploit the DE circuit to obtain one additional advantage. The passbands which are even multiples of f_0 can also be eliminated in a DE circuit [2]. To put it simply, when the frequency of the input is an even multiple of f_0, the input will be the same after a time interval of $T_0/2$ ($T_0 = 1/f_0$). So, if we charge a capacitor using one terminal of the input for a certain time (d), we can discharge it by connecting it to the other terminal of the input after time interval of $T_0/2$ for the same time duration (d).

When the input frequency is odd multiple of f_0, then after time interval of $T_0/2$ it will be negative of what it was before. The capacitor charge will add up instead of getting subtracted. Using this simple idea, we can eliminate the pass bands at even harmonics. The DE 4-path filter is shown in Fig. 3.7.

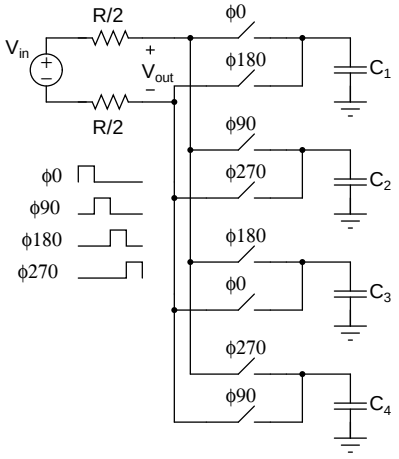

Figure 3.7: 4-path DE switched-RC N-path filter

To obtain the exact expression of the transfer function, one may analyze this LPTV system using state space concept. The references [2], [6] and [5] were helpful in deriving these equations. The expression of the transfer function is given as follows: [2]

$$V_{out}(f) = \sum_{n=-\infty}^{\infty} H_n(f) V_{in}(f - nf_s),$$

$$H_n(f) = \sum_{k=0}^{N-1} H_{n,k}(f),$$

$$H_{n,k}(f) = \frac{e^{-j2\pi n f_s \sigma_k}}{1 + j\frac{f}{f_{rc}}} \times [\frac{1 - e^{-j2\pi n f_s \tau_k}}{j2\pi n} + \frac{1 + e^{j2\pi[(f-nf_s)(\frac{T_s}{2} - \tau_k) - nf_s\tau_k]}}{2\pi \frac{f_{rc}}{f_s}} G_{0,k}(f)], \tag{3.23}$$

$$G_{0,k}(f) = -\frac{e^{j2\pi(f-nf_s)\tau_k} - e^{-2\pi f_{rc}\tau_k}}{e^{j2\pi\frac{f-nf_s}{f_s}} + e^{-2\pi f_{rc}\tau_k}} \times \frac{1}{1 + j\frac{f-nf_s}{f_{rc}}}$$

The expression is quite intimidating and is difficult to interpret. So we resort to the method we developed for analyzing SE circuits and details have been worked out in Appendix A. The expression for the zeroth sideband is given as follows:

$$H_0(f) \approxeq \frac{1}{1 + j2\pi(f - f_0)R\hat{C}} \tag{3.24}$$

where $\hat{C}$ equals $\frac{C}{N|P_1^*|^2}$.

3.3.2 Simulation Result

We have used the same component values used in [2] to realize the 4-path BPF . The value of the resistance R=100Ω, capacitor C=50pF and switching frequency f_0=500MHz as given in thesis. The duty cycle of the switches was slightly less than 0.25. Fig. 3.8 shows the comparison of the transfer function obtained using the model we developed and from simulation. We see that our model correctly describes the behavior of the filter except for the points where the transfer function gives a maximum or a minimum. It was shown in [2] that the simulator's output does matches with the exact transfer function as specified in eq. (3.23). The code for generating the theoretical model is given in Appendix C. The deviation of the exact transfer function from our model is not understood and is left as a scope for future work.

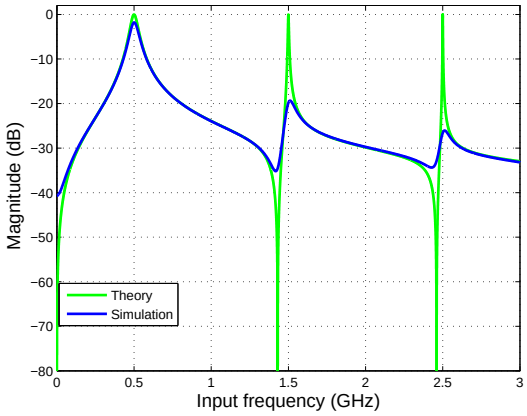

Figure 3.8: Comparison of $H_0(f)$ between theory and simulation results of the 4-path DE filter

3.4 Effect of Non Idealities in the Circuit

We have seen how N-Path filter provides a highly selective passband. But this trait will get impaired if the non-idealities are not handled carefully. We would like to point out two important non-idealities that could harm our transfer function.They are the non zero switch resistance and mismatches in the

components network. Other non-idealities like the imbalance multiphase clocking and thermal noise are not mentioned here and a discussion on them can be found in [2].

3.4.1 Switch Resistance

The effect of switch resistance is actually quite easy to model. The switch resistance can be thought of as a series resistance and can be taken outside in the similar manner the series resistance R was taken in Fig. 3.1.

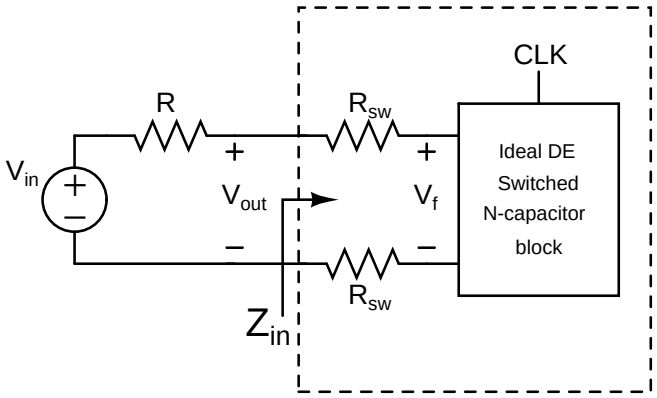

Figure 3.9: DE N-path filter with switch resistance

From Fig. 3.9, the output voltage is given as follows:

$$V_{out}(f) = \frac{2R_{sw}}{2R_{sw}+R}V_{in}(f) + \frac{R}{2R_{sw}+R}V_f(f) \tag{3.25}$$

Where $V_f(f)$ is the output assuming that the resistance seen by the ideal DE switched N-capacitor block is $R+2*R_{sw}$. As we know that during odd multiples of switching frequency ($(2n+1)f_0$), the looking in impedance is high, there is no effect of switch resistance but when we go far away from those frequencies, the impedance is very small and thus, making $V_f(f)$ very low . Then from eq. 3.25:

$$V_{out}(f) = \frac{2R_{sw}}{2R_{sw}+R}V_{in}(f) \tag{3.26}$$

The above equation tells us that the gain in the undesired band has risen. The effect of switch resistance can be reduced by increasing the source impedance R. The effect of switch resistance is shown in the Fig. 3.10.

For R_{sw}= 3, $H_0(f) = \frac{2R_{sw}}{2R_{sw}+R} = \frac{6}{106}$ = -25 dB

For R_{sw}= 6, $H_0(f) = \frac{2R_{sw}}{2R_{sw}+R} = \frac{12}{112}$ = -19.4 dB

These values are close to the $H_0(f)$ obtained from the circuit simulator at DC and other frequencies far away from the odd multiples of f_0.

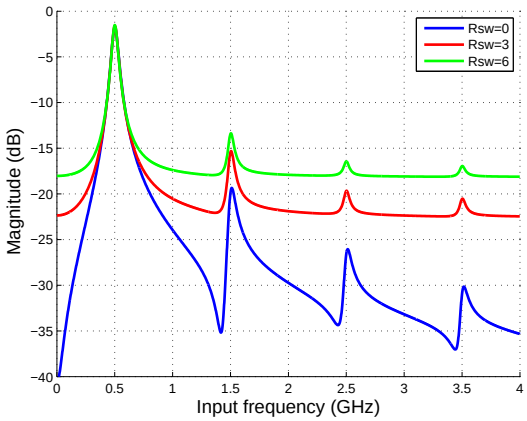

Figure 3.10: Effect of switch resistance

3.4.2 Mismatches in Capacitors

The distinguishing feature of the N-Path network over other LPTV systems is the cancellation of the sidebands which are not a multiple of the number of paths (N). This feature relies on cancellation upon summation of output of each path. Now if there are mismatches in components, i.e if the capacitors or switch resistance differ in each path then this feature will be lost. These sidebands will cause undesired signals to fold back to our desired band. For instance, if H_1 (f) is not zero then the input signal at $2f_0$ will appear as a signal at f_0 and will interfere with actual signal at f_0. This is a potential problem and so, matching between the paths should be paid attention.

CHAPTER 4

Design of 6-Path SE BPF

4.1 Selection of Components

We have used the single ended model discussed in the previous chapter to design the filter. We started with a choice of number of paths as 6. To generate 6 phase clock we have used the Arduino-Uno micro-controller using the CTC mode [7]. In this mode a counter is continuously compared with a register and generates an interrupt when the match occurs. After generating the interrupt, the value of the counter gets cleared and again the comparison starts. So, to a realize 6 phase clock, each of frequency f_0 we have to generate interrupt at a frequency $6f_0$. Arduino-Uno works at a clock of 16MHz. Let's say that a reasonable choice of counter compare register is 32. Then we can generate interrupt to a maximum rate of 50KHz. For this choice, the center frequency will be around 8KHz. As our system heavily relies on the accuracy of the clocks, we have chosen the center frequency to be 3.03KHz (timeperiod equals $55\mu s$). We first chose our bandwidth to be 10.5Hz. To find the values of the components, we have used the formula for bandwidth from eq. 3.21. One choice of the value of R and C is 3.18KΩ and $1\mu F$. It was mentioned earlier that the value of the output at the center frequency is 0.8dB below the theoretical value. Please note that the drop of 0.8dB depends on the number of path and an approximate value of this drop is given in eq. 3.22. So, instead of finding 3dB bandwidth we should find 3.8dB bandwidth. Using the above choice of values of R and C we get the 3.8dB bandwidth of 18Hz which was close to the bandwidth measured from the response of the circuit simulator. As the objective was to just observe the BPF behavior in practice, we have gone ahead with this choice of R and C value.

We have chosen 4066 as the analog switch as it was easy to obtain locally. From the datasheet of 4066 IC [8], the on resistance doesn't vary much with the input voltage for a supply voltage of 10V or above. So, the supply voltage was chosen to be 10V. As the input signal to the switch will take both positive and negative values, the power supply should be $\pm 5V$. Having a 10V power supply brings one problem into the picture. The output given by Arduino-Uno which acts as a clock to the switch is 5V relative to its ground but for normal operation the control signal of the switch should be VDD(+5) for on and VSS(-5) for off. One simple fix is to amplify Arduino's output using a comparator. I have connected the ground of Arduino and VSS of the switch to -5V. So the off voltage of the clock will appear at -5V

and the on voltage will appear at 0V. I have used LM339 to accomplish the task of amplification. The LM339 was given $\pm 5V$ power supply and the reference value for comparison was set to -2.5V using a voltage divider circuit.

For the entire system we have used -5V,0V(ground) ,5V power supply. The input was applied with reference to the ground using an Agilent function generator and the output was measured using a Tektronix DSO . The schematic is shown in Fig. 4.1.

4.2 Measurement and Results

The DSO captures only 2500 points and we have to ensure that the sidebands lie on a bin for taking the DFT. Moreover we have limited choice over sampling rate (f_s). As the bandwidth of our BPF is 18Hz, we must have data points which can show that the output has fallen by 3dB. For that we must have frequencies at intervals of atleast 10Hz from f_0 to fall on a frequency bin while taking the DFT. This will force the maximum sampling rate to be 25KHz which can also be provided by the DSO. We are not done yet. As the output will contain other sidebands we have to ensure that they don't alias with our desired signal. For the frequency at 3.03KHz, the smallest harmonic that can alias back to desired signal is the 2499^{th} one. We assume that in practice the magnitude of this harmonic is too small to be considered. So 25KHz seems to be a good choice for our purpose. For the input frequencies (f_{in}) other than f_0, the output will contain frequencies at f_{in} +mf_0. And if we take frequencies close to $f_0$then the output will contain frequencies approximately at (m+1)f_0 which don't alias back. So, 3.03KHz and 25KHz turn out to be decent choice of center frequency and sampling rate for measurement. As we also want to measure the sidebands, it is important to understand the mathematics behind it which is given in Appendix B.

Fig. 4.2(a) compares the experimental result with the ideal case obtained using the circuit simulator. Though the output obtained from the experiment shows BPF behavior, it deviates slightly from the ideal case. The bandwidth has now increased which could mean either the resistance or the capacitance has decreased. The deviation could not be due to switch resistance as it would instead make the response sharper. After measuring the values of capacitors, it was observed that most of the capacitors were around 850nF. So simulation was run with all the capacitors set to 850nF and the result is shown in 4.2(b). The experimental result matches almost perfectly with the simulated one. The code for plotting the sidebands is given in Appendix C

Fig. 4.3a shows the comparison between the sidebands which are multiples of 6. And in Fig. 4.3b

we have plotted all sidebands except the non zero multiples of 6. As mentioned in Appendix B, we cannot find the magnitude of the non-dominant sidebands at input frequency of f_0. So in the plot of 4.3b, we have not inserted any value for the non dominant sideband at f_0 but we have joined the data points.

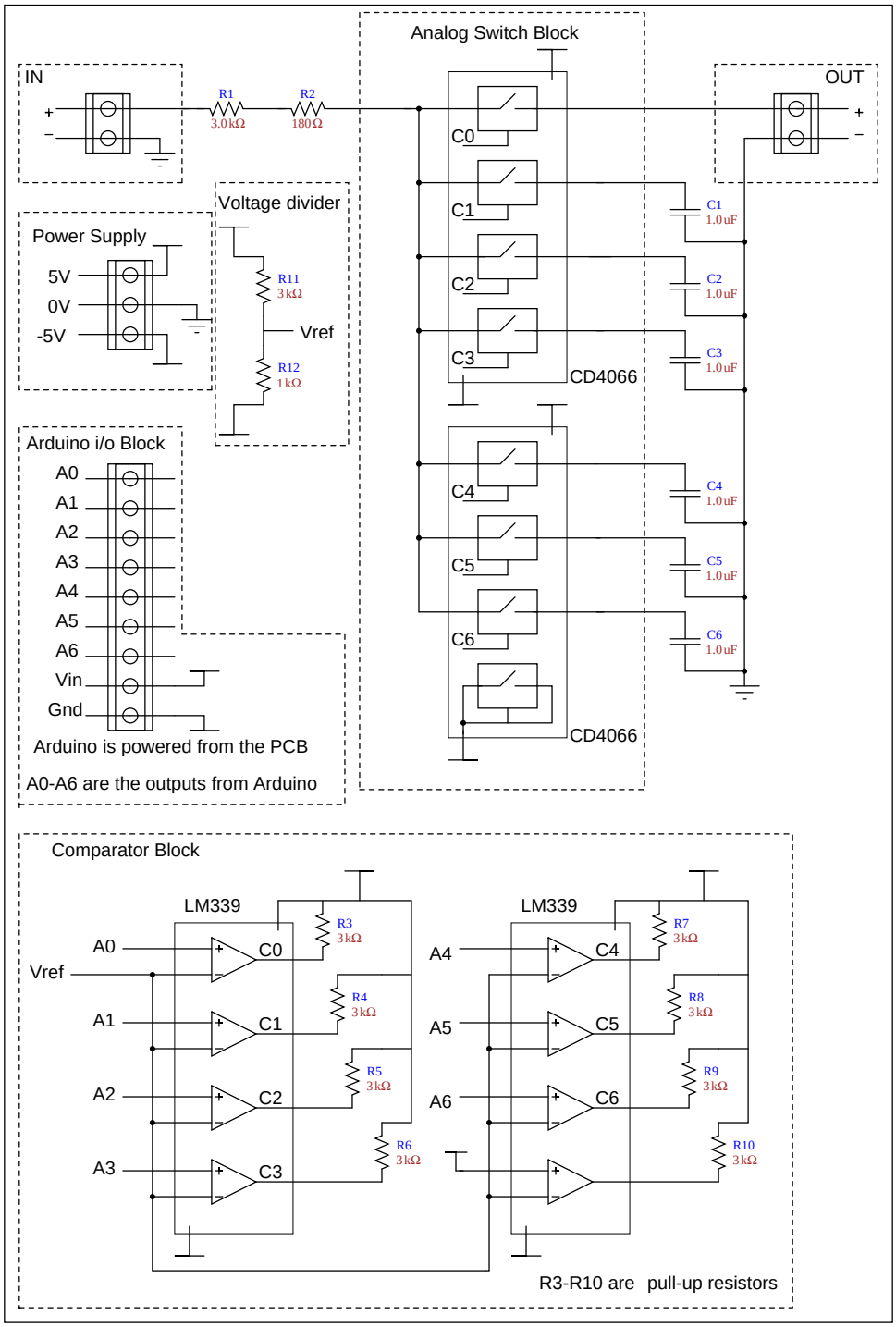

Figure 4.1: Schematic of the 6-path BPF

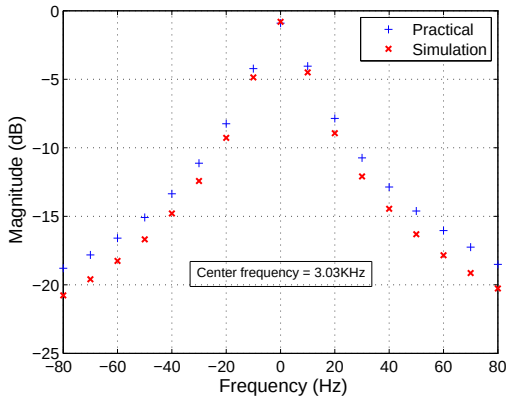

(a) Ideal case

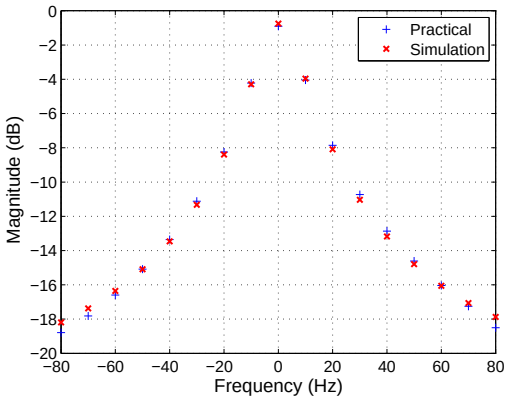

(b) Capacitors in the simulator reduced to 850nF

Figure 4.2: Comparison of the zeroth sideband between the simulated and experimental

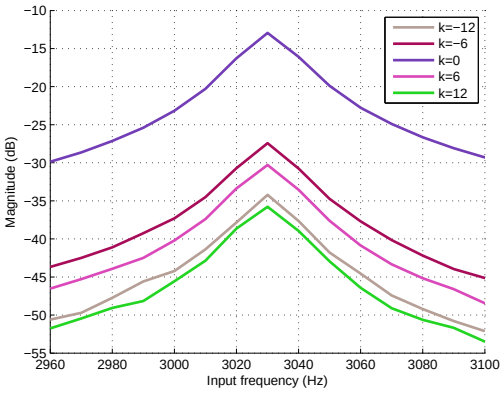

(a) Dominant sidebands in the output

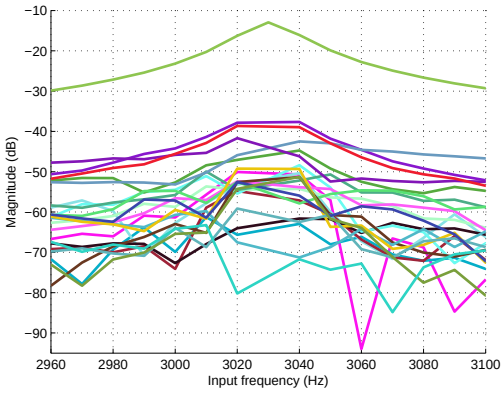

(b) Comparison of all non dominant sidebands with the zeroth sideband

Figure 4.3: Output Spectrum

CHAPTER 5

Conclusion and Scope of Future Work

We have successfully built a BPF using the theory we have developed in the thesis. Designing a high Q BPF filter doesn't seem a big challenge now. However, we were unable to explain why the deviation between our model and the exact expression of the transfer function occurs whenever there is a maximum or a minimum. This makes the calculation of the 3dB bandwidth using our model to go wrong. A simple way to manage this problem is to find the approximate value of the response at the center frequency using the formula we presented and then find the 3dB bandwidth from the value.

There is another class of filters called the pseudo-N-path filter which claims to surpass the N-Path filter in terms of rejection of the undesired sidebands. An introduction to the pseudo-N-path filters can be found in the references [9] and [10]. We encourage the interested readers to go ahead and explore the pseudo-N-path filter concept.

Appendices

APPENDIX A

Derivation of transfer function of DE BPF

The behavior of DE circuit can be understood by determining the looking in impedance of the block shown in Fig. A.1. Following the names given to the node voltages and current in Fig. A.1, we can find the relation between the input current source and the output voltage as follows:

$$i_1(t) = i(t).(p(t) - p(t - \frac{T_0}{2})) = i(t).\hat{p}(t) \tag{A.1}$$

Where p(t) and $\hat{p}$(t) are given in the Fig. A.2.

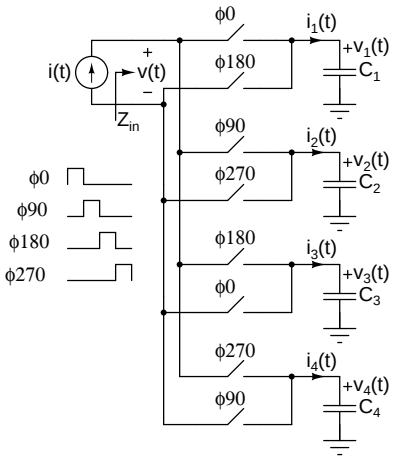

Figure A.1: Z_{in} of switched N-capacitor block

$$i_2(t) = i(t).(p(t - \frac{T_0}{4}) - p(t - 3\frac{T_0}{4})) = i(t).\hat{p}(t - \frac{T_0}{4}) \tag{A.2}$$

Similarly,

$$i_3(t) = i(t).(\hat{p}(t - \frac{T_0}{2})) \tag{A.3}$$

$$i_4(t) = i(t).(\hat{p}(t - 3\frac{T_0}{4}) \tag{A.4}$$

Denoting the Fourier transform of the voltages $v_n(t)$ and currents $i_n(t)$ by $V_n(f)$ and $I_n(f)$, the relation between them is: (assuming C_1=C_2=C_3=C_4=C)

$$V_n(f) = \frac{1}{j2\pi fC}.I_n(f) \tag{A.5}$$

The potential of the positive and negative terminal of the output voltage are:

$$v_+(t) = v_1(t).p(t) + v_2(t).p(t - T_0/4) + v_3(t).p(t - T_0/2) + v_4(t).p(t - 3T_0/4) \tag{A.6}$$

$$v_-(t) = v_3(t).p(t) + v_4(t).p(t - T_0/4) + v_1(t).p(t - T_0/2) + v_2(t).p(t - 3T_0/4) \tag{A.7}$$

$$v_{out}(t) = v_+(t) - v_-(t) = \sum_{i=1}^{4} v_i(t).\hat{p}(t - (i-1)\frac{T_0}{4}) \tag{A.8}$$

From the general input-output relation given in eq. (2.8):

$$V_{out}(f) = \sum_{k=-\infty}^{\infty} F_k(f)I(f - kNf_0) \tag{A.9}$$

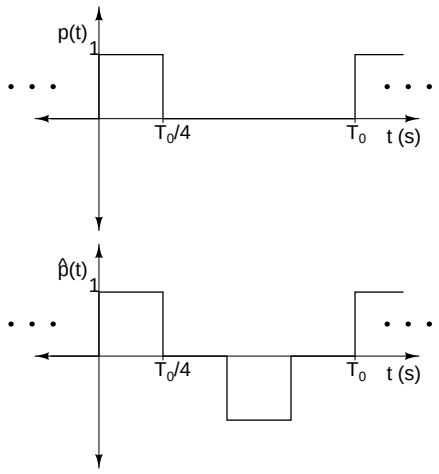

Figure A.2: p(t) and $\hat{p}$(t)

$$F_k(f) = N \sum_{l=-\infty}^{\infty} \hat{P}_{KN-l} \hat{P}_l A(f - lf_0) \tag{A.10}$$

where, $A(f) = \frac{1}{j2\pi(f-lf_0)C}$. Because of the antisymmetric shape of $\hat{p}$(t) , its Fourier series coefficients vanish for even values. From here we can obtain the expression for H_0(f) by following the method used in the SE case and is given by:

$$H_0(f) = \frac{1}{1 + j2\pi(f - f_0)R\hat{C}} \tag{A.11}$$

where $\hat{C}$ equals $\frac{C}{N|\hat{P}_1|^2}$. Please note that the expression contains $\hat{P}_1$ and not P_1 like in the case of SE circuit.

APPENDIX B

Measurement of Sidebands

For an LPTV system, the Fourier transform of the output in terms of input is given by the following [11]

$$V_{out}(\omega) = \sum_{n=-\infty}^{\infty} \hat{H}_n(\omega - n\omega_0) V_{in}(\omega - n\omega_0) \tag{B.1}$$

Where $\hat{H}_n(\omega)$ are the *aliasing transfer functions.* We have changed the notations of input, output, frequency of the LPTV system and the aliasing transfer function from the ones used in the reference [11] to avoid unnecessary confusion. We have already seen the expression of V_{out} in terms of harmonic transfer function and is given as follows:

$$V_{out}(\omega) = \sum_{n=-\infty}^{\infty} H_n(\omega) V_{in}(\omega - n\omega_0) \tag{B.2}$$

By comparison of the above two equations,

$$H_n(\omega) = \hat{H}_n(\omega - n\omega_o) \tag{B.3}$$

When we apply a sinusoid at a frequency f_{in}, the output we get is given by:

$$V_{out}(f) = \sum_{n=-\infty}^{\infty} \hat{H}_n(f - nf_0)[\delta(f - f_{in} - nf_0) + \delta(f + f_{in} - nf_0)] \tag{B.4}$$

We have applied a cosine signal to avoid dealing with 1/j factor when using a sine signal, and frequency domain analysis instead of angular frequency domain and neglected the factor of 1/2. For the sake of understanding let's say that output contains terms only from n = -2 to n =2. After expanding each term, in the output spectrum we get:

- $\hat{H}_0(f_{in})$ at f_{in}
- $\hat{H}_0(-f_{in})$ at $-f_{in}$

- $\hat{H}_1(f_{in})$ at f_0+ f_{in}
- $\hat{H}_1(-f_{in})$ at f_0 - f_{in}
- $\hat{H}_2(f_{in})$ at 2f_0+ f_{in}
- $\hat{H}_2(-f_{in})$ at 2f_0 - f_{in}
- $\hat{H}_{-1}(f_{in})$ at -f_0+ f_{in}
- $\hat{H}_{-1}(-f_{in})$ at -f_0 - f_{in}
- $\hat{H}_{-2}(f_{in})$ at -2f_0 + f_{in}
- $\hat{H}_{-2}(-f_{in})$ at -2f_0 - f_{in}

Our goal is to measure $\hat{H}_k(f_{in})$. The question arises, how to measure $\hat{H}_k$ when k is negative? For this we have to revisit the definitions of what these ATF truly are. From [11] , these $\hat{H}_k$ are the Fourier series coefficient of the time varying transfer function $\hat{H}(t,\omega)$. And it can easily be shown that:

$$\hat{H}_{-k}(\omega) = (\hat{H}_k(-\omega))^* \tag{B.5}$$

So, $|\hat{H}_{-m}(f_{in})|$ which appears at -mf_0+f_{in} can be obtained from $|\hat{H}_m(-f_{in})|$ which appears at mf_0-f_{in}. So, k^{th} sideband for the input frequency f_{in} can be obtained by taking the DFT of the output and finding out the component at -kf_0-f_{in} when k is negative and kf_0 +f_{in} when k is positive. However, when f_{in} equals f_0 these ATF overlap. For instance, both $H_0(f_0)$ and $H_2(-f_0)$ occur at f_0 and we cannot find by taking the DFT what the values of the ATF are. To find the value of $H_0(f_0)$ in our experiment we have assumed that $H_2(-f_0)$ is negligible. We have also assumed that the sidebands which are multiple of 6 also dominate over other sidebands.

APPENDIX C

Codes

```
%This code plots the transfer function of the DE BPF using the model we
%developed
clear all;
close all;


f=0:5000:4e9; % freq range
R=100;
C=50e-12;


%Numerator of terms corresponding to l = 1, 3, 5
P1=8/(pi^2);
P3=8/(9*pi^2);
P5=8/(25*pi^2);

%f0 = 500MHz
%Denominators of the terms corresponding to l = 1, 3, 5 -1 -3 -5
D1=i*2*pi*(f-500e6)*C;
D2=i*2*pi*(f-1500e6)*C;
D3=i*2*pi*(f-2500e6)*C;
D4=i*2*pi*(f+500e6)*C;
D5=i*2*pi*(f+1500e6)*C;
D6=i*2*pi*(f+2500e6)*C;

% N & D give the numerator and denominator of the trasfer function
% respectively
N=P1*(D2.*D3.*D5.*D6).*(D1+D4)+P3*(D1.*D3.*D4.*D6).*(D2+D5)+P5*(D1.*D2.*D4.*D5).*(
    D3+D6);
D=R*(D1.*D2.*D3.*D4.*D5.*D6)+N;
plot(f/1e9,20*log10(abs(N./D)),'g','LineWidth',2);
grid on;
ylim([-60 0]);
xlabel('Frequency (GHz)');
```

```
ylabel('Magnitude (dB)');
```

Listing C.1: Plotting theoretical transfer function

```
%This code takes the output of the DSO stored as .csv file for each input
%frequency and generates a matrix containing the magnitude in dB of each
%sideband for each input frequency.
clear all;
f0 = 3.03e3 ; % Center freq
fs = 25e3; % Sampling rate

k = 12; %Number of sidebands
f_sweep = 17;%Frequency sweep range 2950 to 3110 Hz at intervals of 10Hz.

%Store the bin number corresponding to sideband at a particular frequency
HTF_pos = zeros([1,2*k+1]);

%Generate a Matrix. For each frequency we store the magnitudes of all the
%sidebands in row corresponding to that frequency.
HTF = zeros(f_sweep,2*k+1);

addcsv = '.csv';

for j1 = 1:f_sweep
    f = 2.95e3 + 10*(j1-1); %input freq
    %Find the location of sideband in the DFT spectrum and store this in
    %HTF_pos
    for j2 = -k:k
        if j2 < 0
            f_sideband =  abs(-1*j2*f0 -f) ;
        else
            f_sideband =  j2*f0 +f ;
        end
        fft_pos = mod(f_sideband,fs);
        if fft_pos > 12500
            fft_pos = fs - fft_pos;
        end
        HTF_pos(j2+k+1) = fft_pos/10;
    end
    %The output data for freq at f say 3.03K was stored as 303.csv
    fname = int2str(f/10);
```

```
38      file = strcat(fname,addcsv);
39      f=csvread(file,0,4,[0 4 2499 4]);
40      N=2500;
41      y=f';
42      n=0:N-1;
43      w=0.5*(1-cos(2*pi*n/N)); %Hann window
44      y_win=y.*w;
45      y_fft=abs(fft(y))/N;
46      y_win_fft=abs(fft(y_win))/N;
47
48      for j3 = 1:2*k+1
49          HTF(j1,j3) = dbv(y_win_fft(HTF_pos(j3)+1));
50      end
51
52  end
53  hold all;
54  fin = 2950:10:3110 ;
55  for j4 = 1:5
56      sb = -12 + 6*(j4-1); %sb -> sideband
57      sb = sb + 13;
58     plot(fin,HTF(:,sb),'Color',[rand rand rand],'LineWidth',2)
59  end
60  xlim([2960 3100]);
61  grid on;
62  xlabel('Input frequency (Hz)');
63  ylabel('Magnitude (dB)');
64  legend('k=-12','k=-6','k=0','k=6','k=12');
```

Listing C.2: Plotting the dominant Sidebands

REFERENCES

[1] L. E. Franks and I. W. Sandberg. An alternative approach to the realization of network transfer functions: The n-path filter. *Bell Sys. Tech. J.*, 39:1321–1350, Sep. 1960.

[2] Amir Ghaffari. *Switched-RC Radio Frequency N-path filters*. PhD thesis, University of Twente, 2013.

[3] Upamanyu Madhow. *Fundamentals of Digital Communication*. Cambridge University Press, 2008.

[4] P. P. Vaidyanathan. *Multirate Systems And Filter Banks*. Prentice-Hall, 1993.

[5] M. C. M. Soer and et al. Unified frequency-domain analysis of switched-series- passive mixers and samplers. *Circuits and Systems I: Regular Papers, IEEE Transactions on*, 57:2618–2631, 2010.

[6] T. Ström and S. Signell. Analysis of periodically switched linear circuits. *Circuits and Systems, IEEE Transactions on*, CAS-24:531–541, Oct. 1977.

[7] Atmega 328 datasheet. URL http://www.atmel.com/Images/doc8161.pdf.

[8] Analog switch 4066 datasheet. URL http://www.ti.com/lit/ds/symlink/cd4066b.pdf.

[9] H. Wupper. A modified n-path filter suited for practical realization. *Circuits and Systems, IEEE Transactions on*, 21:449–456, May 1974.

[10] A. Fettweis. A solution to the balancing problem in n-path filters. *Circuit Theory, IEEE Transactions on*, 18:403–405, May 1971.

[11] Fei Yuan. *Noise, Sensitivity and Distortion Analysis of Switched Analog Circuits*. PhD thesis, University of Waterloo, 1999.

[12] Amir Ghaffari, Eric A.M. Klumperink, and Bram Nauta. A differential 4-path highly linear widely tunable on-chip. *Radio Frequency Integrated Circuits Symposium (RFIC), IEEE*, pages 299–302, May 2010.